Comparing the Thermo-Physical Properties of Rice Husk and Rice Straw as Feedstock for Thermochemical Conversion and Characterization of their Waste Ashes from Combustion

Xiwen Yao,[a] Kaili Xu,[a,*] and Yu Liang [b]

The thermogravimetric characterization and gas emission properties during the pyrolysis of rice husk (RH) and rice straw (RS) were compared, and the properties of waste rice husk ash (RHA) and rice straw ash (RSA) from the combustion process were investigated. The results showed that the pyrolysis of RH and RS followed a four-step mechanism. Comparing the emission properties of small molecule bio-syngas in the pyrolysis of these two biomass wastes implied that RS was more suitable for use as feedstock for thermochemical conversion. Chemical and phase analysis results indicated that the RSA was rich in K, Ca, and P and had good potential for use as a soil amendment or as a material for silicate ceramics. The RHA was rich in SiO_2 and could be an ideal silica source for silicon compound preparation or a pozzolan source for blended cement concrete production. Morphology analysis on the ash samples revealed that the high content of alkali metals may cause the higher agglomeration tendency of RSA with respect to RHA. The contrast in pore properties of biomass char wastes isolated from the ashes indicated that the char wastes recovered from RHA would be better used as a low-cost precursor in activated carbon production.

Keywords: Rice husk; Rice straw; Thermal pyrolysis; Gaseous products; Ash properties; Applications

*Contact information: a: School of Resources and Civil Engineering, Northeastern University, Shenyang 110819, PR China; b: College of Information Science and Engineering, Northeastern University, Shenyang 110819, PR China; *Corresponding author: neu_kailixu@126.com*

INTRODUCTION

The development of renewable and clean energy sources has drawn increasing attention due to the depletion of fossil fuel reserves and other environmental issues (Said *et al*. 2014). As an alternative fuel, biomass wastes have been regarded as one of the major assets for renewable energy, and they can be provided mainly by local energetic resources. Moreover, in comparison with petroleum-based products, biomass-based fuels produce less net CO_2 emissions because the CO_2 generated from biomass thermal utilization can be used and recycled by plants during the growing process (Mikulčić *et al.* 2014). Consequently, there are a variety of prominent techniques to transform biomass wastes into clean energy and sustainable fuels, and interest in producing energy and fuels from biomass has grown tremendously in the last decades (Yao *et al.* 2016). Globally, well-renowned technologies for bio-energy recovery from biomass wastes include thermochemical processes such as combustion, gasification, and pyrolysis. Thermal pyrolysis is the initial step of biomass thermal utilization, and it plays a key role during the thermal conversion. After transient high thermalization, large amounts of carbon-rich wastes called biomass ash are produced.

Rice is an important cereal crop that is widely planted worldwide; global annual production of rice is approximately 10.8 million tons (Paethanom and Yoshikawa 2012). In China alone, the yield of rice reached more than 2.08 million tons in 2015, according to the China Statistical Yearbook (2015). During the processing of rice, the main biomass wastes or byproducts are rice husk (RH) and rice straw (RS). According to Zhou *et al*. (2011), the value of the agricultural biomass product-residue coefficient for rice is approximately 0.623. Thus, in China in 2015, the estimated yield of agricultural wastes (including RH and RS) from rice processing was approximately 1.30 million tons. These data are tremendous given Chinese production volume of available biomass wastes, indicating an immense potential for bio-energy production.

Several recent studies on the pyrolysis of RH or RS have focused on the effects of pyrolysis conditions (such as heating rate, atmosphere, particle size, *etc*.) on the thermogravimetric characterization of RH or RS (Worasuwannarak *et al*. 2007; Sun *et al*. 2010; Chen *et al.* 2014; Gao *et al*. 2015; Moliner *et al*. 2016). For example, Moliner *et al*. (2016) studied the thermal and thermo-oxidative characterization of rice straw for its use in energy valorization processes, as well as the influence of carrier gas (Ar and O_2) on its pyrolysis. Gao *et al*. (2015) investigated the effects of alkali and alkaline earth metals on N-containing species released during RS pyrolysis. There also is much research concentrating on the dynamics models that predict the kinetics during pyrolysis (Arora *et al.* 2009; Cai *et al.* 2013; Mishra and Bhaskar 2014; Wang *et al.* 2016). These findings indicated that the thermochemical reactions occurring during the pyrolysis could be well defined and described mathematically.

Though there are numerous studies investigating the pyrolysis behaviors of agricultural wastes from rice that deal with the relationship between thermogravimetric characterization and pyrolysis conditions, only a few studies have addressed the emission characteristics of gas products released during RH and RS pyrolysis (Worasuwannarak *et al*. 2007; Fu *et al*. 2010; Zhai *et al.* 2015). Moreover, the characterization of the waste rice husk ash (RHA) and rice straw ash (RSA) generated during biomass thermal conversion and their utilizations for the development of biomaterials have not been thoroughly investigated. In addition, due to the economic and population growths in China, rice demand is expected to remain strong in the coming decades. The incessant generation of RHA and RSA will represent a serious problem if these solid waste materials cannot be disposed of properly. For instance, the disposal of RHA in landfills or open fields may cause serious environmental and human health-related problems due to the low bulk density of RHA (Pode 2016). Even so, different biomass ashes can be used as precursor materials in various fields, based on their properties. So far, several studies have been conducted on the characterization of biomass ash (Xu *et al*. 2012; Kilpimaa *et al.* 2013; Vassilev *et al.* 2013), yet the properties of the waste ashes from the RH and RS wastes under similar thermochemical conditions have received limited attention.

In this study, the RH and RS were selected as typical agricultural wastes for pyrolysis. The thermogravimetric characterization and gas emission characterization during the pyrolysis of these two biomasses were investigated using a thermogravimetric (TG) analyzer coupled with a mass spectrometer (MS) in a He atmosphere. The typical non-condensable gas products (primarily CO, CO_2, CH_4, H_2, and H_2O) were gathered and analyzed continuously during the pyrolysis process for facilitating the further utilization of RH and RS in bio-syngas production and comparing their potential availability as thermochemical conversion feedstock. Furthermore, to guide the efficient utilization of the waste RHA and RSA, their primary properties that serve as predictors of suitability in

various applications were comprehensively investigated using a series of qualitative and quantitative analysis methods.

EXPERIMENTAL

Biomass Materials

The RH and RS samples used in this study (from a rural area of Shenyang, China) are common and widely available in China. Prior to experiments, all the biomass materials were oven-dried at 105 ± 0.5 °C for 24 h, grinded and pulverized using a high speed rotary cutting mill, and sieved with a 100-mesh sieve. The samples that passed through the sieve (less than 0.154 mm in size) were collected in a closed vessel and retained to be analyzed.

The volatile matter (VM), fixed carbon (FC), and ash yield (A) of the received biomass materials were measured by a 5E-MACIII Infrared Speediness Coal Analyzer (Kaiyuan Apparatus Co., Changsha, China). The moisture (M) was determined by a Sartorius Moisture Analyzer IMA 30 (Sartorius Lab Instruments Co., Goettingen, Germany). Final analysis was performed quantitatively by a Vario MACRO Elemental Analyzer (Elementar, Frankfurt, Germany). The low heating value (LHV) of the used materials was measured by IKA Calorimeter System C2000 (Guangzhou, China). Table 1 illustrates the general characterization of the prepared biomass materials, which is the average of three measurements. All the values showed a good reproducibility with the standard deviation of < 2.0%, and the precision of the measurements was 0.5%.

Table 1. General Characterization of Biomass Materials (on Air-Dried Basis)

Materials	Proximate Analysis (wt.%)				Ultimate Analysis (wt.%)					LHV (MJ/kg)
	VM	M	FC	A	C	H	O	N	S	
RH	70.82	0.79	13.19	15.20	45.93	5.61	31.29	1.03	0.15	15.28
RS	72.43	1.38	14.37	11.82	43.89	5.18	36.37	1.25	0.11	14.79

Pyrolysis Experiments

The thermogravimetric analysis (TGA) of biomass materials was carried out in a sensitive thermal balance (NETZCH-STA449 F3, Selb, Germany) at a heating rate of 20 °C/min up to a final temperature of 1200 °C. In pyrolysis, high purity helium (99.99%) at a flow rate of 30 mL/min was used as the carrier gas to provide an inert atmosphere for pyrolysis and to remove the gaseous and condensable products, thus minimizing any secondary vapor-phase interactions. The sensitivity was 1 μg and 0.01 °C, and approximately 5 mg of sample was pyrolyzed for each test.

A quadrupole mass spectrometer (QMS 403D, Pfeiffer Vacuum Technology, Selb, Germany) coupled to the thermal balance was employed for the evolved gas analysis. To avoid secondary reactions, the gases released were purged immediately to the mass spectrometer to obtain the evolution curves. The transfer line and gas cell were preheated to 200 °C to avoid cold spots and to prevent the condensation of semi-volatile products. The signals for mass numbers of 2, 16, 18, 28, and 44 were continuously detected and then converted to the emission intensities of H_2, CH_4, H_2O, CO, and CO_2, respectively, by referring to the calibration curves constructed using the standard gases. The mass spectrometer was operated in EI mode with 70 eV of electron energy.

Preparation of Biomass Ash

There are no specific standards available for biomass ash preparation in China. By comparison of biomass ashes obtained under different temperatures, literature (Vassilev *et al*. 2013; Du *et al*. 2014) suggested that 600 °C was the most appropriate temperature to exactly determine the properties of biomass ash and to perform ash analysis in industrial applications. Thus, the ashing temperature was set at 600 °C according to the ASTM E1755-01 standard (2015). These prepared biomass samples (particle size < 0.154 mm) were put in a Muffle furnace (SX2-15-12, Dongtai Shuangyu Instruments Co. Ltd., Jiangsu, China) and kept for 2 h at 600 °C. The storage interval of this furnace was 1 °C, and the atmosphere was free air.

Here it is worth mentioning that biomass pyrolysis and biomass combustion are two types of thermochemical processes, which are both used for converting biomass to energy. Generally speaking, pyrolysis refers to the incomplete thermal degradation which leads to the production of coal tars, fuel gases, and condensable liquids. In the strictest sense, pyrolysis must be performed in the absence of oxygen; however, this term is now used in a broader connotation, to describe the chemical changes caused by the action of heat (Baray *et al*. 2014). In the combustion process, oxidation is substantially complete in a one-step process (Kilpimaa *et al.* 2013), but in the pyrolysis process, the chemical energy of biomass is converted into value-added products through many steps. Besides, pyrolysis is considered as the initial step of biomass thermal utilization and one of the promising thermo-chemical conversion routes, which plays a vital role in biomass conversion.

Determination of Ash Characterization

In the present study, the chemical composition of ash was obtained by using X-ray fluorescence (XRF; ZSX100e, Rigaku Co., Tokyo, Japan). The main crystalline minerals present in ash were qualitatively determined by an X-ray diffractometer (XRD; X'Pert PRO, PANalytical B.V., Almelo, Netherlands) with Cu Kα radiation (λ = 0.15406 nm) at a scan rate of 0.02°/s. Scanning electron microscopy (SEM) (Ultra Plus, Carl Zeiss Co. Ltd., Oberkochen, Germany) and energy dispersive X-ray (EDX) (Genesis, Edax DX-4) at an accelerating voltage of 20 to 30 kV were employed to obtain more information on the ash, such as ash morphology, agglomeration characteristics, and the surface composition of ash powders. Prior to the SEM-EDX analysis, the ash samples were gold-coated to make them electrically conductive.

The carbon content of separated ash wastes was analyzed quantitatively by using Vario MACRO Elemental Analyzer (Elementar, Frankfurt, Germany), and the specific surface area, pore size, and pore volume were measured by nitrogen adsorption measurement using a Quantachrome Autosorb-6B analyzer (Boynton Beach, FL, USA). First, the char wastes were degassed for 12 h under vacuum at 200 °C prior to analysis to remove any adsorbed species, then the analysis was carried out with nitrogen as adsorbate.

RESULTS AND DISCUSSION

Thermal Decomposition Characteristics

Pyrolysis can convert agricultural wastes efficiently into a variety of eco-friendly and value-added products, but predicting the product quality usually depends on the

thermogravimetric characterization of the feed materials. Thus, the pyrolysis characteristics of the prepared biomass materials were investigated by thermogravimetric analysis. The thermogram curves of RH and RS heated at 20 °C/min in helium are shown in Fig. 1.

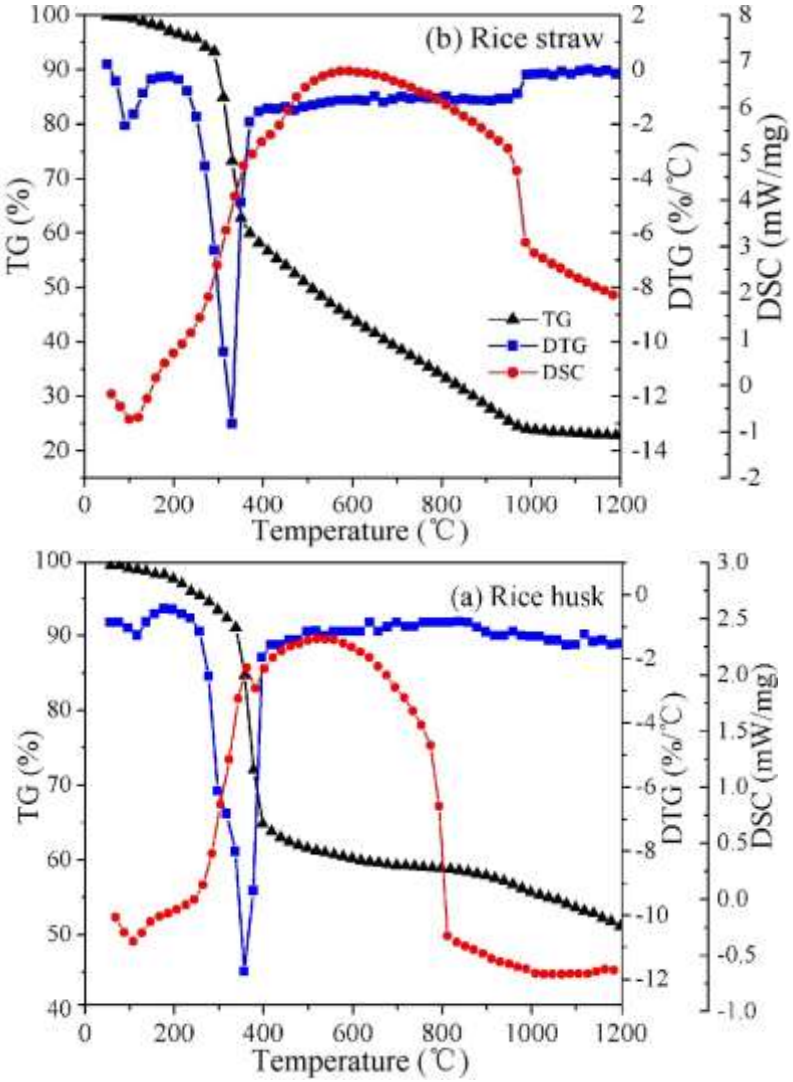

Fig. 1. Thermogram curves of (a) rice husk and (b) rice straw

The thermal degradation of these two agricultural wastes showed stepwise mechanisms, and mainly occurred in four steps that can be explained from their chemical composition. The first weight loss (below 210 °C) was mainly due to the loss of moisture. The major weight loss (within 210 to 400 °C) that followed was due to the thermal degradation of hemicellulose and cellulose. The third stage was from 400 to 900 °C, in which the slow weight loss was mostly related to the pyrolysis of lignin in biomass. The last stage took place beyond 900 °C and continued until the final temperature, and there was no remarkable weight loss in this stage. These results were basically consistent with Wang *et al*. (2008), who reported that among the three components of biomass (cellulose, hemicellulose, and lignin), hemicellulose is the easiest one to be pyrolyzed, followed by cellulose, while lignin is the most difficult.

The weight loss of RH and RS recorded as a function of temperature are shown in Figs. 1a and 1b, respectively. The results indicate a total weight loss around 50% for RH (Fig. 1a) and around 70% for RS (Fig. 1b). Initially, the degradation rates were slow, but there was a distinct shoulder peak between 70 and 140 °C. Simultaneously, an endothermic peak occurred at around 100 °C, indicating the energy adsorbed during the volatilization of moisture from biomass samples.

With regards to the DTG curves, a rapid degradation of biomass clearly occurred when the temperature was higher than 210 °C. The weight loss between 210 and 400 °C was mostly caused by the evolution of volatile components from the pyrolysis of biomass, which greatly contributed to the total weight loss of biomass. Moreover, as observed from the DTG curves, the pyrolysis of RH had the maximum weight loss rate at approximately 355.8 °C, while the maximum weight loss rate of RS occurred at approximately 331.6 °C. Above 400 °C, an insignificant weight loss occurred at a slower degradation rate when compared with the weight loss within 210 and 400 °C.

TG and DTG patterns are used to establish thermal degradation profiles, and some vital parameters for evaluating the thermal performance of biomass can be derived from these profiles. To compare the thermal behaviors of various biomasses, a comprehensive devolatilization parameter has been defined by Zeng *et al.* (2013) as follows,

$$D = \frac{(dw/dt)_{max}\,(dw/dt)_{mean}}{T_s T_{max} \Delta T_{1/2}} \quad (1)$$

where $(dw/dt)_{max}$ is the maximum weight loss rate, $(dw/dt)_{mean}$ is the mean weight loss rate, T_s is the starting temperature for volatile release and weight loss, T_{max} is the temperature of maximum weight loss rate, $\triangle T_{1/2}$ reflects the temperature of full width at half maximum for the main peak of DTG curves, and D reflects the volatile release characteristic index.

The main pyrolysis characteristic parameters determined from TG and DTG profiles are summarized in Table 2. The starting degradation temperature (T_s) of RH was 227 °C, which was higher than that of RS (204 °C).

Table 2. Characteristic Parameters from the Thermal Degradation Curves

Materials	Starting temperature (T_s) (°C)	Peak temperature (T_{max}) (°C)	Temperature of full width at half maximum ($\triangle T_{1/2}$) (°C)	Maximum weight loss rate $(dw/dt)_{max}$ (%/min)	Mean weight loss rate $(dw/dt)_{mean}$ (%/min)	Volatile release characteristic index (D)	Total weight loss (W_t) (%)
RH	227	355.8	48.3	-14.00	-0.85	3.07×10^{-6}	51.05
RS	204	331.6	53.4	-13.36	-1.17	4.36×10^{-6}	69.96

The T_s is a key indicator of the thermal stability of biomass; the higher the T_s, the better the thermal stability (Sharma and Ghoshal 2010). Hence, the thermal stability of RH was better than that of RS, which in turn suggested that the pyrolysis of RS occurred with relatively more ease. Moreover, the total weight loss of RS (69.96%) was much greater than that of RH (51.05%), which indicated that the residual char yield of RS was less. Furthermore, the volatile release characteristic index (D) value of RS was also greater than that of RH.

Mass Spectrometry (MS) Evolution Profiles

To better understand the pyrolysis behaviors of RH and RS as gasification and pyrolysis feedstock, the gas emission properties during pyrolysis were investigated by mass spectrometry. Figure 2 exhibits the emission intensities of typical non-condensable gaseous products (consisting primarily of CO, CO_2, CH_4, H_2, and H_2O) with temperature increases during the pyrolysis of biomass.

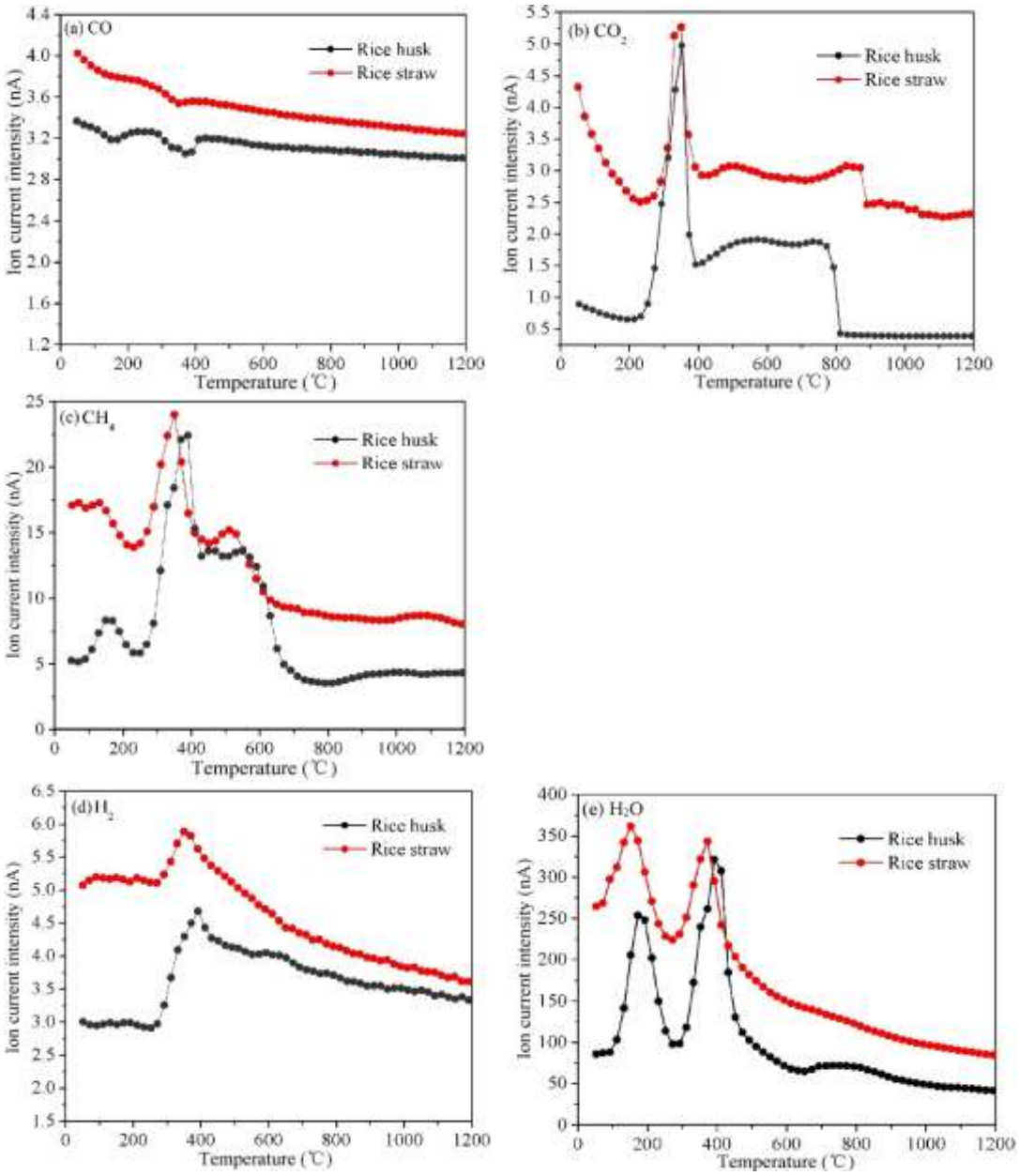

Fig. 2. Evolution of light gaseous products with increasing temperature during the pyrolysis

The gas releasing profiles of RS exhibited a pattern similar to those of RH. However, due to the higher contents of volatile matter, moisture, and fixed carbon in RS biomass, the intensities of CO, CO_2, CH_4, H_2, and H_2O during the pyrolysis of RS were

all higher than those of RH. The higher intensities indicated that the RS pyrolyzed more thoroughly than RH under similar pyrolysis conditions.

The emission of CO took place at a fairly high emission intensity with no distinct releasing peaks in the whole pyrolysis process of biomass (Fig. 2a). Moreover, with the temperature exceeding 600 °C, the intensity of CO emission remained almost constant. Meng *et al*. (2013) reported that the CO was mainly released with the cracking of carbonyl (C–O–C) and carboxyl (C=O) in the pyrolysis of hemicellulose throughout the entire temperature range, and that of lignin at high temperatures (> 600 °C).

As shown in Fig. 2b, CO_2 was mainly emitted between 100 and 800 °C, with one distinct peak. At low temperatures (< 500 °C), the abundant presence of C=O chemical groups in the hemicellulose was suggested to favor CO_2 production, while at high temperatures (> 500 °C) lignin pyrolysis contributed a small portion (Yang *et al*. 2007). CO_2 emission beyond 800 °C decreased dramatically with an increase in temperature, due to the fact that the CO_2 was mainly released from volatile matters below 800 °C.

Unlike the emission of CO_2, there were two peaks representing CH_4 emission (Fig. 2c). The first peak with lower intensity was at approximately 180 °C, while the second one shifted towards higher temperature zones (300 to 450 °C). The second peak was much stronger and sharper than the first one due to the small amount of char wastes (less than 10 wt.% of the original sample) derived from the low temperature stage. Lignin is rich in methoxyl-O-CH_3 chemical groups, so the CH_4 emission was most likely produced through the cracking of methoxyl-O-CH_3 during the pyrolysis of lignin below 600 °C. This finding agreed with Liu *et al*. (2008).

H_2 was predominantly released between 300 and 600 °C (Fig. 2d). The emission intensity of H_2 increased when the temperature increased from 300 °C and reached the maximum peak at approximately 400 °C. This result indicated that high H_2 emission was obtained from the pyrolysis of cellulose and hemicellulose, which are pyrolyzed below 400 °C (Wu *et al*. 2013). As a note, the high emission of hydrogen mentioned here refers to the relatively high emission intensity of H_2, which is qualitative and not quantitative. Beyond 400 °C, the H_2 emission decreased up to 1200 °C, suggesting that the pyrolysis of lignin above 400 °C generates a relatively lower H_2 emission when compared with the pyrolysis of other components of biomass.

Similar to CH_4 emission, the H_2O emission also had two conspicuous peaks (Fig. 2e). The first one was below 210 °C, and the second one was between 210 and 500 °C, corresponding well with the thermogravimetric data of the first two pyrolysis stages in Fig. 1. The H_2O emission in the temperature range of 100 to 500 °C was mainly from the evolution of bulk water, bound water, and crystallization water in mineral substance. Above 500 °C, the H_2O from the cracking or reaction of oxygen functional groups decreased slowly with the increment of temperature.

Chemical and Phase Analysis of Biomass Ash

The elemental analysis results of biomass ashes obtained by XRF are depicted in Table 3. All elements were translated into oxides (Cl converted to equivalent oxygen) and then normalized. The XRD analysis results indicated the qualitative presence of crystalline minerals in the ash samples, as shown in Fig. 3.

Table 3. Chemical Composition of Ash Wastes Determined by XRF (wt.%)

Samples	SiO_2	K_2O	Na_2O	CaO	MgO	SO_3	P_2O_5	Fe_2O_3	Al_2O_3	TiO_2	MnO	Cl
RHA	94.79	1.86	0.39	0.75	0.55	0.09	0.23	0.86	0.36	0.02	0.02	0.08
RSA	73.26	13.46	0.93	4.46	2.14	2.41	1.94	0.49	0.25	0.05	0.04	0.57

The oxides in RHA and RSA can be categorized into acidic oxides (SiO_2, Al_2O_3, SO_3, and P_2O_5, *etc*.) and basic oxides (K_2O, CaO, MgO, Na_2O, Fe_2O_3, *etc*.) according to their acidic and basic capacity. The proportions of alkaline and alkaline earth metal elements (commonly including K, Na, and Ca) in RSA were much higher than those of RHA. Moreover, the Cl content of RSA was also higher than that of RHA. According to Vamvuka and Zografos (2004), the Cl element could serve as a facilitator of alkali vaporization, which may result in a serious vaporization of alkali metals in the form of chlorides, such as KCl and NaCl. Öhman *et al*. (2000) suggested that high contents of alkaline and alkaline earth metals and related compounds could easily cause slagging, fouling, and corrosion problems for thermochemical conversion equipment. Thus, from the economic and environmental point of view, it can be concluded that RSA can cause slagging, fouling, and corrosion problems with more relative ease than does RHA.

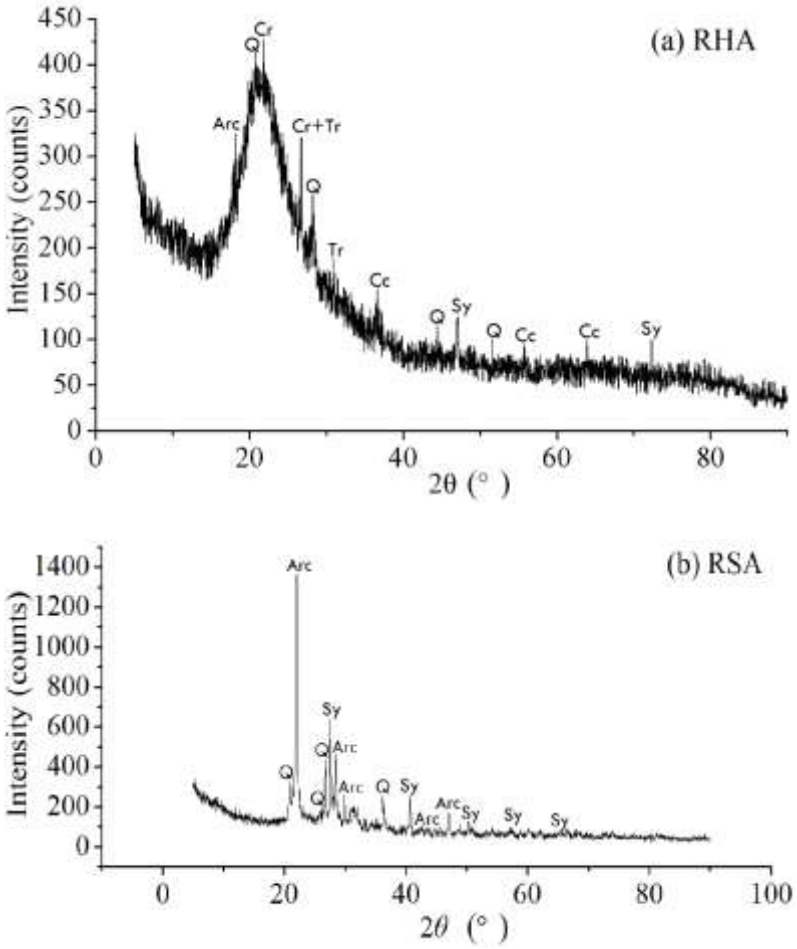

Fig. 3. XRD patterns of (a) RHA and (b) RSA (abbreviations: Arc, arcanite [K_2SO_4]; Cc, calcite [$CaCO_3$]; Cr, cristobalite [SiO_2]; Q, quartz [SiO_2]; Sy, sylvite [KCl]; Tr, tridymite [SiO_2])

The composition results in Table 3 also indicate that SiO_2 was predominant in these two ash samples. It was especially high in RHA, where the proportion of SiO_2 reached up to 94.79%, much higher than that of RSA. This result can also be confirmed by XRD analysis of RHA (Fig. 3b), which indicated the presence of silica primarily in the form of cristobalite, quartz, and tridymite (the major crystalline minerals in RHA). Hence, from the ash utilization point of view, RHA would be an ideal SiO_2 source for the preparation of silicon compounds. In addition, the high silica content gives RHA the potential for use as a pozzolan material for blended cement concrete production.

In RSA, the content of K_2O was much higher than other oxides except for SiO_2. These levels were further supported by the results of XRD analysis in Fig. 3b, which exhibited the presence of potassium, mainly in the forms of arcanite (K_2SO_4) and sylvite (KCl), and the presence of silica, in the form of quartz (SiO_2), as the major components in RSA. After investigating sunflower husk ash (SHA) as a raw material for ceramic products, Quaranta *et al*. (2011) demonstrated that the elements Si, K, Ca, and Mg were highly beneficial for the production of dense bodies used in traditional ceramic industries. Because the elemental composition of RSA was similar to that of SHA, RSA with relatively high contents of SiO_2 (73.26%), K_2O (13.46%), CaO (4.46%), and MgO (2.14%) could be used as a precursor for ceramic products in the construction industry. Moreover, the biomass ash from RS was enriched with typical nutrient elements (mostly K, Ca, and P), indicating the potential use of RSA as a soil amendment or a crude fertilizer to improve the physical and biological properties of agricultural soil.

SEM-EDX Analysis of the Ash

Prior to morphology analysis, a metal spraying treatment (gold/carbon coating for conductivity) of biomass ash was necessary because the electric conductive performance of biomass ash is poor. After the metal spraying treatment, the detailed morphology information and the surface composition of RHA and RSA were obtained by SEM-EDX analysis. Figure 4 exhibits the SEM images for RHA (Figs. 4a and 4b) and RSA (Figs. 4c and 4d) formed at 600 °C, illustrating the ash morphology and agglomeration characteristics. The spectra of EDX spot analyses in points a-d of Figs. 4a-d are shown in Figs. 5a-d, and all the original EDX data are presented in Table 4.

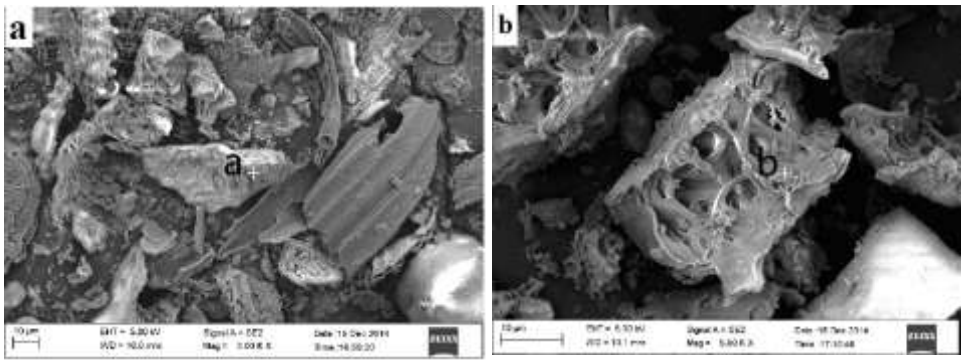

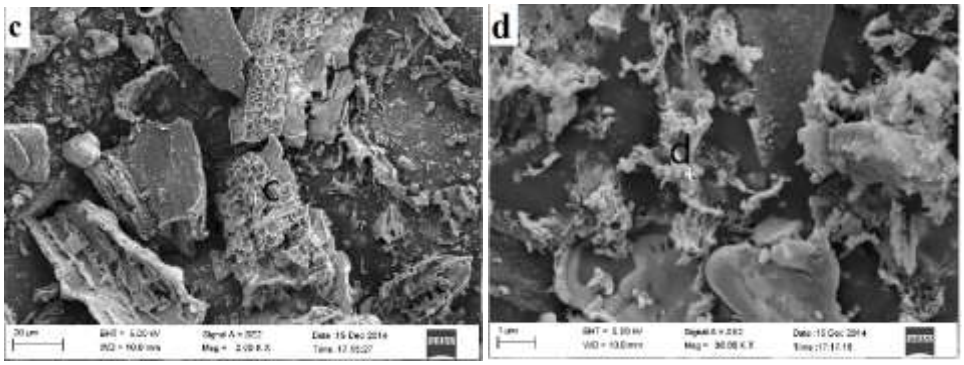

Fig. 4. SEM images formed at 600 °C for (a and b) RHA and (c and d) RSA

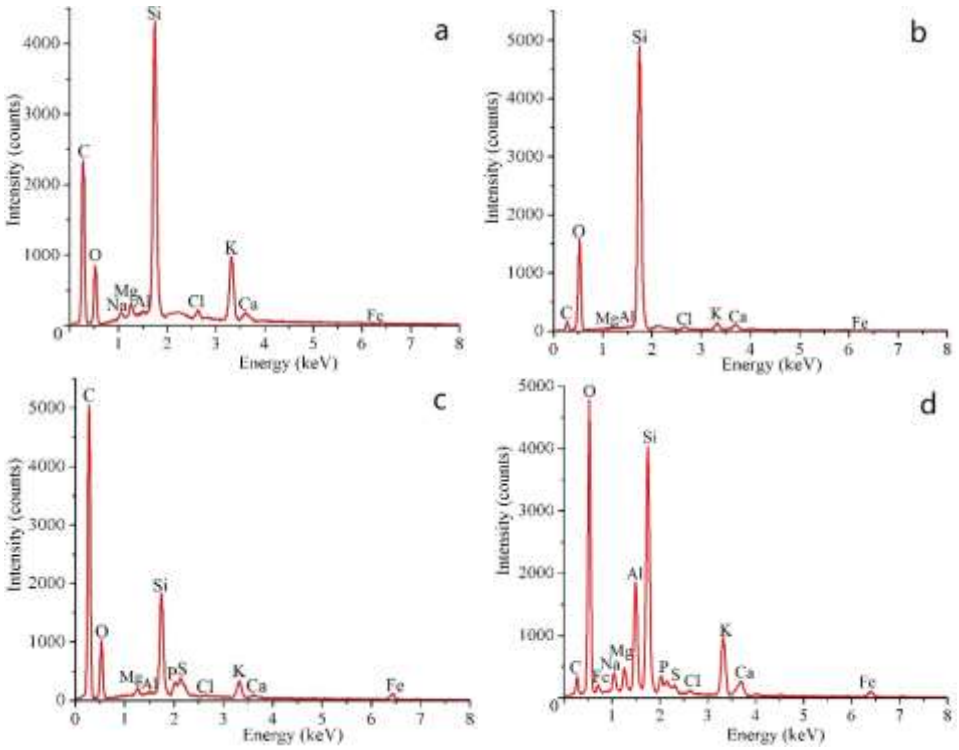

Fig. 5. Spectra of EDX spot analyses in points a-d of Figs. 4a-d

As seen in Fig. 4, there were some leaf shape particles in RHA (Fig. 4a), while in RSA (Fig. 4c) more seriously broken ash particles were clearly observed, indicating that under the same burning conditions the original fiber structure of RS was more easily damaged. As shown in Table 5, the predominant elements on the ash surface mainly included C, O, Si, K, and Ca, while lesser amounts of Na, Mg, Al, Cl, Fe, *etc*. were also detected. In addition, both the spectrum of point a (Fig. 5a; on the surface of RHA powders) and that of point c (Fig. 5c; on the surface of RSA powders) had a high carbon content. These high carbon levels indicated that some unburned carbon wastes still existed in the ashes combusted at 600 °C on account of inadequate combustion of biomass fuels.

Table 4. Results of EDX Spot Analyses in Points a-d of Figs. 4a-4d (wt.%)

Point	C	O	Na	Mg	Al	Si	P	S	Cl	K	Ca	Fe
a	50.16	18.46	0.33	0.73	0.08	25.31	-	-	0.52	1.64	2.65	0.12
b	13.67	37.09	-	0.03	0.07	45.89	-	-	0.08	0.46	2.15	0.29
c	66.05	20.72	-	0.43	0.09	8.95	0.53	0.26	0.23	2.56	0.17	0.01
d	7.69	46.60	1.61	1.57	7.60	18.38	1.17	0.57	0.42	8.81	2.48	3.09

Figure 4b shows the interior details of a typical RHA particle. A closer examination of Fig. 4b shows that this typical ash particle contained a great deal of large voids. In addition, the external surface of this typical RHA particle was thick, while its internal surface was relatively thin, accompanied by a crisscrossed slab and pore structure in the middle. The EDX results of point b (Fig. 5b and Table 4) on the internal surface of this particle showed that the contents of Si and O were, respectively, as high as 45.89% and 37.09%, further confirming that SiO_2 was the major mineral substance in RHA.

As can be seen in Fig. 4d, there were some amorphous particles and irregularly shaped floccules in RSA, revealing the adhesion and slight caking of small particles. This result also reveals that RSA had a higher agglomeration tendency than RHA under the same burning conditions. The EDX results of point d (Table 4 and Fig. 5d) on the surface of these floccules showed that the carbon content was only 7.69%, while the contents of Si and O were, respectively, as high as 18.38% and 46.60%. These percentages reveal that much amorphous SiO_2 was present on the surface of floccules. Moreover, after comparing the morphology of RHA with that of RSA from the ash agglomeration point of view, it can be concluded that the slagging or agglomeration of RSA was much more serious with respect to RHA. The above results were consistent with the composition and phase results determined by the earlier XRF and XRD analyses, further validating the accuracy of the measurements in this study.

Pore Properties Analysis

The pore properties of char wastes isolated from the prepared biomass ashes were investigated. The char wastes in RHA and RSA were separated by using the of density gradient centrifugation (DGC) technique (Maroto-Valer *et al*. 1999). The pore properties vital for char wastes as a natural low-cost adsorbent in terms of carbon content, specific surface area, pore size, and pore volume were determined (Table 5). All the values presented good reproducibility with the standard deviation of < 2.0%, and the precision of the measurements was 0.5%.

Table 5. Pore Texture Parameters and Carbon Content of Char Wastes

Biomass Char Wastes	Carbon Content (wt.%)	Specific Surface Area (m^2/g)	Pore Size (Å)	Pore Volume (cm^3/g)
RHA	82.26	205.32	17.73	0.145
RSA	65.37	27.69	11.26	0.109

In both cases, the char wastes isolated from RHA had a higher specific surface area than RSA. This difference remained true for carbon content, pore size, and pore volume. These results were basically the same as the results of the earlier SEM analysis, which clearly exhibited that the RHA powders possessed more large voids than the RSA

powders. Moreover, the contrast of pore properties in char wastes from RHA and RSA, respectively, indicated that the char wastes recovered from waste RHA were more suitable for use as a potential source for producing activated carbon. Considering the increasing demand for cheap sources of adsorbents, the pore properties of RHA make it a potential low-cost precursor material for the production of adsorbents.

Summary about Characterization and Possible Applications of the Ash

The results of XRF analysis for RSA showed the high contents of metallic oxides (primarily including K_2O, CaO, and MgO) in the ash, and this indicates the suitability and availability of RSA as raw materials for silicate ceramics. Also, the relatively high contents of potassium, calcium, and phosphorus make it possible for the RSA to be used as a kind of crude fertilizer in agricultural soils. XRD results showed the transformation behavior of crystalline structures of RHA and RSA. Larger amount of SiO_2 compounds in the form of cristobalite, quartz, and tridymite was identified in RHA, which reveals that the silica-rich RHA can be an ideal silica source for silicon compound preparation. Besides, the high silica content makes RHA have the potential to be used as pozzolan materials for the production of blended cement concrete in the building industry.

In addition, the results of pore properties analysis showed that the carbon content of the char wastes isolated from RHA was quite high, indicating that these char wastes recovered from RHA can be potentially used as low-cost precursors for activated carbon production. Furthermore, both RHA and RSA in this research were found to be devoid of toxic metals, thus there exist a possibility for them to be employed for the applications of clarification, separation, and decontamination in various industries.

CONCLUSIONS

1. In this study, the thermo-physical properties of agricultural wastes from RH and RS during pyrolysis were investigated. The characterization of waste RHA and RSA suitable for use in applications was also determined.
2. Thermogravimetric analysis of RH and RS indicated that their decomposition had a four-step mechanism. The characteristic parameters of T_s, T_{max}, $(dw/dt)_{mean}$, and D of RH were found to have greater values in comparison with those of RS, while the $\triangle T_{1/2}$ and W_t values of RS were much higher than those of RH.
3. A comparison of the emission properties of the typical non-condensable gases (such as CO, CO_2, CH_4, H_2, and H_2O) during the pyrolysis suggested that RS was more suitably used as a feedstock for thermochemical conversion in bio-syngas production.
4. XRF and XRD results indicated that the RSA with rich potassium, calcium, and phosphorus had potential for use as a soil amendment or as a raw material for silicate ceramics. The RHA rich in SiO_2 could be an ideal silica source for silicon compound preparation, as well as a pozzolan for blended cement concrete production in the construction industry.
5. Scanning electron microscopy-energy dispersive X-ray analysis on ash samples indicated that the high content of alkali metals caused the higher agglomeration tendency of RSA with respect to RHA. The contrast in the pore properties of char

wastes separated from RHA and RSA revealed that the char wastes from RHA were more suitable for use as a low-cost precursor for activated carbon production.

ACKNOWLEDGMENTS

The authors are grateful for the support of Rural Energy Comprehensive Construction Found of the Ministry of Agriculture of China (Grant. No. 2015-36).

REFERENCES CITED

Arora, S., Kumar, M., and Dubey, G. P. (2009). "Thermal decomposition kinetics of rice husk: Activation energy with dynamic thermogravimetric analysis," *Journal of the Energy Institute* 82(3), 138-143. DOI: 10.1179/014426009X12448168550109

ASTM E1755-01 (2015). "Standard test method for ash in biomass," ASTM International, West Conshohocken, USA.

Baray, G. M. R., Silva, P. M. M., Melendez, Z. M., Gutierrez, J. S., Guzman, V. V., Lopez, O. A., and Collins-Martinez, V. (2014). "Thermogravimetric study on the pyrolysis kinetics of apple pomace as waste biomass," *International Journal of Hydrogen Energy* 39(29), 16619-16627. DOI: 10.1016/j.ijhydene.2014.06.012

Cai, J. M., Wu, W. X., and Liu, R. H. (2013). "Sensitivity analysis of three-parallel-DAEM-reaction model for describing rice straw pyrolysis," *Bioresource Technology* 132, 423-426. DOI: 10.1016/j.biortech.2012.12.073

Chen, D. Y., Zhou, J. B., Zhang, Q. S., Zhu, X. F., and Lu, Q. (2014). "Torrefaction of rice husk using TG-FTIR and its effect on the fuel characteristics, carbon, and energy yields," *BioResources* 9(4), 6241-6253. DOI: 10.15376/biores.9.4. 6241-6253

China Statistical Yearbook (2015). National Bureau of Statistics of China, Beijing: Statistics Press of China. (in Chinese)

Du, S. L., Yang, H. P., Qian, K. Z., Wang, X. H., and Chen, H. P. (2014). "Fusion and transformation properties of the inorganic components in biomass ash," *Fuel* 117(B), 1281-1287. DOI: 10.1016/j.fuel.2013.07.085

Fu, P., Hu, S., Xiang, J., Li, P. S., Huang, D., Jiang, L., Zhang, A. C., and Zhang, J. Y. (2010). "FTIR study of pyrolysis products evolving from typical agricultural residues," *Journal of Analytical and Applied Pyrolysis* 88(2), 117-123. DOI: 10.1016/j.jaap.2010.03.004

Gao, P., Xue, L., Lu, Q., and Dong, C. Q. (2015). "Effects of alkali and alkaline earth metals on N-containing species release during rice straw pyrolysis," *Energies* 8(11), 13021-13032. DOI: 10.3390/en81112356

Kilpimaa, S., Kuokkanen, T., and Lassi, U. (2013). "Characterization and utilization potential of wood ash from combustion process and carbon residue from gasification process," *BioResources* 8(1), 1011-1027. DOI: 10.15376/biores.8.1.1011-1027

Liu, Q., Wang, S. R., Zheng, Y., Luo, Z. Y., and Cen, K. F. (2008). "Mechanism study of wood lignin pyrolysis by using TG–FTIR analysis," *Journal of Analytical and Applied Pyrolysis* 82(1), 170-177. DOI: 10.1016/j.jaap.2008.03.007

Maroto-Valer, M. M., Taulbee, D. N., and Hower, J. C. (1999). "Novel separation of the differing forms of unburned carbon present in fly ash using density gradient centrifugation," *Energy and Fuels* 13(4), 947-953. DOI: 10.1021/ef990029s

Meng, A. H., Zhou, H., Qin, L., Zhang, Y. G., and Li, Q. H. (2013). "Quantitative and kinetic TG-FTIR investigation on three kinds of biomass pyrolysis," *Journal of Analytical and Applied Pyrolysis* 104, 28-37. DOI: 10.1016/j.jaap.2013.09.013

Mikulčić, H., von Berg, E., Vujanović, M., and Duić, N. (2014). "Numerical study of co-firing pulverized coal and biomass inside a cement calciner," *Waste Management and Research* 32(7), 661-669. DOI: 10.1177/0734242X14538309

Mishra, G., and Bhaskar, T. (2014). "Non isothermal model free kinetics for pyrolysis of rice straw," *Bioresource Technology* 169, 614-621. DOI: 10.1016/j.biortech.2014.07.045

Moliner, C., Bosio, B., Arato, E., and Ribes, A. (2016). "Thermal and thermo-oxidative characterisation of rice straw for its use in energy valorisation processes," *Fuel* 180, 71-79. DOI: 10.1016/j.fuel.2016.04.021

Öhman, M., Nordin, A., Skrifvars, B. J., Backman, R., and Hupa, M. (2000). "Bed agglomeration characteristics during fluidized bed combustion of biomass fuels," *Energy and Fuels* 14(1), 169-178. DOI: 10.1021/ef990107b

Paethanom, A., and Yoshikawa, K. (2012). "Influence of pyrolysis temperature on rice husk char characteristics and its tar adsorption capability," *Energies* 5(12), 4941-4951. DOI: 10.3390/en5124941

Pode, R. (2016). "Potential applications of rice husk ash waste from rice husk biomass power plant," *Renewable and Sustainable Energy Reviews* 53, 1468-1485. DOI: 10.1016/j.rser.2015.09.051

Quaranta, N., Unsen, M., Lopez, H., Giansiracusa, C., Roether, J. A., and Boccaccini, A. R. (2011). "Ash from sunflower husk as raw material for ceramic products," *Ceramics International* 37(1), 377-385. DOI: 10.1016/j.ceramint.2010.09.015

Said, N., Daiem, M. M. A., García-Maraver, A., and Zamorano, M. (2014). "Reduction of ash sintering precursor components in rice straw by water washing," *BioResources* 9(4), 6756-6764. DOI: 10.15376/biores.9.4.6756-6764

Sharma, S., and Ghoshal, A. K. (2010). "Study of kinetics of co-pyrolysis of coal and waste LDPE blends under argon atmosphere," *Fuel* 89(12), 3943-3951. DOI: 10.1016/j.fuel.2010.06.033

Sun, S. Z., Tian, H. M., Zhao, Y. J., Sun, R., and Zhou, H. (2010). "Experimental and numerical study of biomass flash pyrolysis in an entrained flow reactor," *Bioresource Technology* 101(10), 3678-3684. DOI: 10.1016/j.biortech.2009.12.092

Vamvuka, D., and Zografos, D. (2004). "Predicting the behaviour of ash from agricultural wastes during combustion," *Fuel* 83(14-15), 2051-2057. DOI: 10.1016/j.fuel.2004.04.012

Vassilev, S. V., Baxter, D., Andersen, L. K., and Vassileva, C. G. (2013). "An overview of the composition and application of biomass ash. Part 1. Phase-mineral and chemical composition and classification," *Fuel* 105, 40-76. DOI: 10.1016/j.fuel.2012.09.041

Wang, G. W., Zhang, J. L., Shao, J. G., Jiang, Y. K., Gao, B., Zhao, D., Liu, D. H., Wang, H. Y., Liu, Z. J., and Jiao, K. X. (2016). "Experiments and kinetic modeling for the oxidative decomposition of herbaceous and wooden residues," *BioResources* 11(2), 4821-4838. DOI: 10.15376/biores.11.2.4821-4838

Wang, G., Li, W., Li, B. Q., and Chen, H. K. (2008). "TG study on pyrolysis of biomass and its three components under syngas," *Fuel* 87(4-5), 552-558. DOI: 10.1016/j.fuel.2007.02.032

Worasuwannarak, N., Sonobe, T., and Tanthapanichakoon, W. (2007). "Pyrolysis behaviors of rice straw, rice husk, and corncob by TG-MS technique," *Journal of Analytical and Applied Pyrolysis* 78(2), 265-271. DOI: 10.1016/j.jaap.2006.08.002

Wu, C. F., Wang, Z. C., Huang, J., and Williams, P. T. (2013). "Pyrolysis/gasification of cellulose, hemicellulose and lignin for hydrogen production in the presence of various nickel-based catalysts," *Fuel* 106, 697-706. DOI: 10.1016/j.fuel.2012.10.064

Xu, W., Lo, T. Y., and Memon, S. A. (2012). "Microstructure and reactivity of rich husk ash," *Construction and Building Materials* 29, 541-547. DOI: 10.1016/j.conbuildmat.2011.11.005

Yang, H. P., Yan, R., Chen, H. P., Lee, D. H., and Zheng, C. G. (2007). "Characteristics of hemicellulose, cellulose and lignin pyrolysis," *Fuel* 86(12-13), 1781-1788. DOI: 10.1016/j.fuel.2006.12.013

Yao, X. W., Xu, K. L., and Li, Y. (2016). "Physicochemical properties and possible applications of waste corncob fly ash from biomass gasification industries of China," *BioResources* 11(2), 3783-3798. DOI: 10.15376/biores.11.2.3783-3798

Zeng, W. Y., Jin, J., Zhang, H., Gao, W. J., Gao, X. Y., Dong, Z., and Meng, L. (2013). "Pyrolysis characteristics and kinetics mechanism of two typical sludge," *Journal of Combustion Science and Technology* 19(6), 544-548. DOI: 10.11715/rskxjs. R201303020

Zhai, M., Zhang, Y., Ge, T. Z., Dong, P., and Zhao, C. J. (2015). "Simulation of a gas-solid flow field in a two-stage rice husk high-temperature pyrolysis and gasification cyclone gasifier," *BioResources* 10(3), 4569-4579. DOI: 10.15376/biores.10.3.4569-4579

Zhou, X. P., Wang, F., Hu, H. W., Yang, L., Guo, P. H., and Xiao, B. (2011). "Assessment of sustainable biomass resource for energy use in China," *Biomass and Bioenergy* 35(1), 1-11. DOI: 10.1016/j.biombioe.2010.08.006

Article submitted: August 18, 2016; Peer review completed: October 23, 2016; Revised version received and accepted: October 25, 2016; Published: November 1, 2016.
DOI: 10.15376/biores.11.4.10549-10564